Infrared Physics & Technology 71 (2015) 285–288

Contents lists available at ScienceDirect

Infrared Physics & Technology

journal homepage: www.elsevier.com/locate/infrared

Spectral modification of array truncation effects in infrared frequency selective surfaces

Jeffrey A. D' Archangel [a], Eric Z. Tucker [b], Glenn D. Boreman [b,*]

[a] CREOL, The College of Optics & Photonics, University of Central Florida, 4304 Scorpius St., Orlando, FL 32816, United States
[b] Department of Physics and Optical Science, University of North Carolina at Charlotte, 9201 University City Blvd., Charlotte, NC 28223, United States

HIGHLIGHTS

- The resonant condition of a square-loop IR FSS is seen to blue-shift upon array truncation.
- The blue-shifting due to truncation is corrected using small changes in the geometry of finite square-loop FSS arrays.
- A measureable diffuse reflectance is observed for the truncated arrays, which is attributed to diffraction.

ARTICLE INFO

Article history:
Received 4 December 2014
Available online 11 May 2015

Keywords:
Frequency selective surfaces
Metamaterials
Metasurfaces
Hemispherical directional reflectance

ABSTRACT

Infrared frequency selective surfaces (FSS) are widely used in quasi-infinite, planar configurations; however, applications for finite arrays exist as well. Here, a square loop infrared FSS was designed with an infinite array resonance near 10 μm when illuminated at 60° off-normal. Along with the quasi-infinite array, a patterned area containing finite arrays of 7×7 square loops of this design was fabricated and characterized to have a resonance which was blue-shifted due to the effects of truncation. To counteract the effects of truncation, two geometrically modified arrays of 7×7 square-loop elements were designed and fabricated to shift the resonant wavelength approximately back to that of the infinite array.

1. Introduction

Infrared frequency selective surfaces (FSS) have been investigated in recent times for their wide range of electromagnetic filtering capability, including the control of spectral properties [1–4] as well as phase [5,6]. For ease of computation, FSS are typically considered infinite in extent. While much of the demonstrated utility of infrared FSS has been well-approximated by infinite arrays, there exist applications where arrays of finite extent on the order of 10×10 unit cells have been implemented. For example, pixel-scale sensors have been populated with FSS elements for spectrally engineered response at infrared [7] and terahertz [8,9] frequencies. Additionally, free-standing flakes of truncated FSS have been demonstrated toward a possible large area, conformal infrared FSS coating [10,11].

When finite arrays of FSS approach lateral dimensions on the order of the design wavelength, the optical response is impacted significantly. Most notably, a blue-shifting of the far-field resonant condition is observed due to reduced mutual coupling of the outermost elements in the truncated arrays [11,12]. The purpose of this current work is to compensate for the spectral shifting of the FSS resonance due to truncation. There are several potential ways to tune the spectral resonance of truncated arrays. At radio frequencies, circuit elements can be inserted into the individual unit cells for local tuning of the array properties [13]. This is not nearly as convenient at infrared frequencies due to the much smaller dimensions required for functionality. Here, an infinite square-loop infrared FSS is designed with an absorptive resonance near 10 μm, when illuminated at 60° off-normal. The off-normal performance was of interest as an extension of a previous work, in which a near-field apparatus was used that required a 60° angle of illumination [12]. Geometric modifications are implemented in 7×7 truncated arrays of the square-loop design in an attempt to mitigate the blue-shifting which occurs upon truncation. Two design modifications are carried out. One design modification implements slightly larger square loops on the border of the truncated arrays, while the other utilizes a graded size increase from the center loop to the border. Both modifications employ the fact that the resonant wavelength of a square loop varies according to its perimeter; the changes are implemented toward the outermost elements of the finite arrays, where the effects of truncation

* Corresponding author.
E-mail address: gboreman@uncc.edu (G.D. Boreman).

http://dx.doi.org/10.1016/j.infrared.2015.04.015
1350-4495/

are most significant. The results are shown experimentally in terms of the specular and diffuse components of the hemispherical directional reflectance.

2. Design

Design and simulation of the baseline, infinite FSS discussed here was carried out in Ansys HFSS, a 3D electromagnetic solver utilizing the finite element method. It is noted that the optical properties of the materials used in the simulations were determined by ellipsometric measurements of samples fabricated using the deposition equipment utilized in this work. The goal of the infinite design was to create a strong absorber at 60° off-normal to act as the baseline for studies on array truncation. The FSS design consisted of Au square loops upon a ZnS standoff layer above a Cr ground plane. A design such as this resonates strongly when a fundamental (dipolar) mode is excited upon the square loops, which is enhanced by the presence of the ground plane and dielectric standoff layer. The infinite FSS design was simulated using the Floquet port method, which considers only a single unit cell and applies the appropriate boundary conditions to assume a planar, infinite array. The design was optimized by parameterization of the loop size, periodicity, and dielectric layer thickness for a strong resonance near 10 μm, at 60° off-normal, for s-polarized excitation. The final dimensions of the design were as follows: the Au loops had an edge length of 1.44 μm, a periodicity of 1.79 μm, a line width of 0.25 μm, and a thickness of 75 nm. The thickness of the ZnS layer was 320 nm and the Cr ground plane was 150 nm.

The truncated arrays were simulated as single finite arrays using s-polarized plane wave excitation and perfectly matched layer boundaries on the external faces of the computational domain. The spectral response in terms of absorbed power was computed from 8 to 12 μm by integrating the volume loss density over the volume which was simulated. Then, this value was normalized to the incident excitation power to obtain the absorptivity. To limit interactions between adjacent arrays, a spacing of 6.35 μm was introduced between them in the fabricated sample. This spacing was determined via simulations to be a distance where significant coupling would not occur between adjacent arrays.

The goal of the modified truncated arrays was to compensate for the blue-shift in resonant wavelength that is observed in finite arrays where the lateral dimensions are on the order of the design wavelength. As a control sample, a baseline design of 7×7 loop arrays with all the square loops identical to that of the original infinite design was both simulated and fabricated. In the modified arrays, geometric alterations of certain unit cells were used to shift the peak wavelength of resonance. Due to a diminished mutual coupling between neighboring unit cell elements, the local effects of array truncation are most significant at the outermost elements in a finite array [12]. For this reason, the design modifications implemented here were concentrated toward the border elements of the 7×7 arrays.

Many possible alterations to the 7×7 arrays were considered and simulated. Two of these designs were chosen for further study because for these it was observed that very small changes in the geometry realized the sought after result of shifting the peak wavelength of resonance. In both cases, the slight modifications were parameterized while simulating the spectral response from 8 to 12 μm until the peak wavelength of resonance was observed to shift to 10 μm. One design implemented slightly larger square loops on the border of the 7×7 arrays; here, an edge length 50 nm larger than the interior loop was observed to yield a resonant wavelength of 10 μm. The other design modification implemented a gradual increase in the loop edge lengths from the center loop to the border loops of the 7×7 arrays. Here, the center loop of each 7×7 array was left unchanged, while each outward ring of loops had a progressive edge length increase of 12.5 nm to yield a resonant wavelength of 10 μm. It is noted that in both cases, only the size of certain square loops was modified, while the rest of the geometry (including the periodicity of the square loops) was the same as the infinite array design.

3. Fabrication and characterization

Fabrication of the quasi-infinite and truncated FSS arrays was carried out using electron-beam lithography and lift-off. The Cr ground plane was deposited by electron-beam evaporation while the ZnS layer was deposited using thermal evaporation. Lithographic patterning of the square loops was performed using PMMA-A7 electron-beam resist. The exposed areas were developed using a solution of equal parts isopropyl alcohol and methyl isobutyl ketone. Metallization of the 75 nm thick Au loops was carried out using electron-beam evaporation, with a 2.5 nm Ti adhesion layer. Lift-off was carried out using Remover-PG, an n-methyl pyrrolidinone solution containing surfactants (Microchem).

Fig. 1 is a collection of false-color scanning electron microscope (SEM) images showing the three 7×7 designs which were fabricated. False-color is implemented because the differences in geometry are not readily observed in monotone images. The top image (a) depicts an unaltered 7×7 array, where all of the loops are sized according to the infinite FSS design. The middle image (b) depicts a 7×7 array where the interior loops are the size of the infinite FSS design and the perimeter loops (shaded in red) have a loop edge length which is 50 nm larger than those in the interior. The lower image (c) depicts a 7×7 array where a graded size increase has been implemented. Here, the center loop is the size of the infinite FSS design, the light blue-shaded loops have an edge length which is 12.5 nm larger, the green-shaded loops have an edge length which is 25 nm larger, and the orange-shaded loops have an edge length which is 37.5 nm larger than the infinite FSS design. It is noted again that in all cases, the space between adjacent finite arrays was 6.35 μm; this spacing was determined in simulations to provide enough fill-factor to yield a strong absorptivity while allowing minimal coupling between adjacent arrays.

Spectral characterization from 8 to 12 μm was carried out using a Surface Optics Corporation SOC-100 hemispherical directional reflectometer. This apparatus utilizes a 2π hemi-ellipsoid reflector, which uniformly illuminates the sample with a blackbody source to measure the hemispherical directional reflectance (HDR). The reflectometer is capable of discriminating between the specular (SDR) and diffuse (DDR) components by implementing a beam-blocker at the angle of specular reflectance, such that the specular and diffuse reflectance sum to equal the HDR and their angular distributions sum to 2π. The reflectometer measures the HDR and DDR directly, such that the SDR is computed as the difference between them. Here, the angle of specular reflectivity was set to 60° off-normal, to coincide with the intended functionality of the FSS design. At 60° off-normal, the interrogation area of the sample is approximately 2.5 mm × 5 mm. The sample was populated with 3 mm × 8 mm patterned areas to ensure they would fill the interrogation area of the characterization apparatus.

4. Results and discussion

The experimental and simulated SDR of the samples patterned in this work, for s-polarized light at 60° off-normal, is shown in Fig. 2. The absorptive optical resonances are observed as dips in the reflectance spectra. As can be seen in the figure, the quasi-infinite array has an experimental resonance at 10.02 μm,

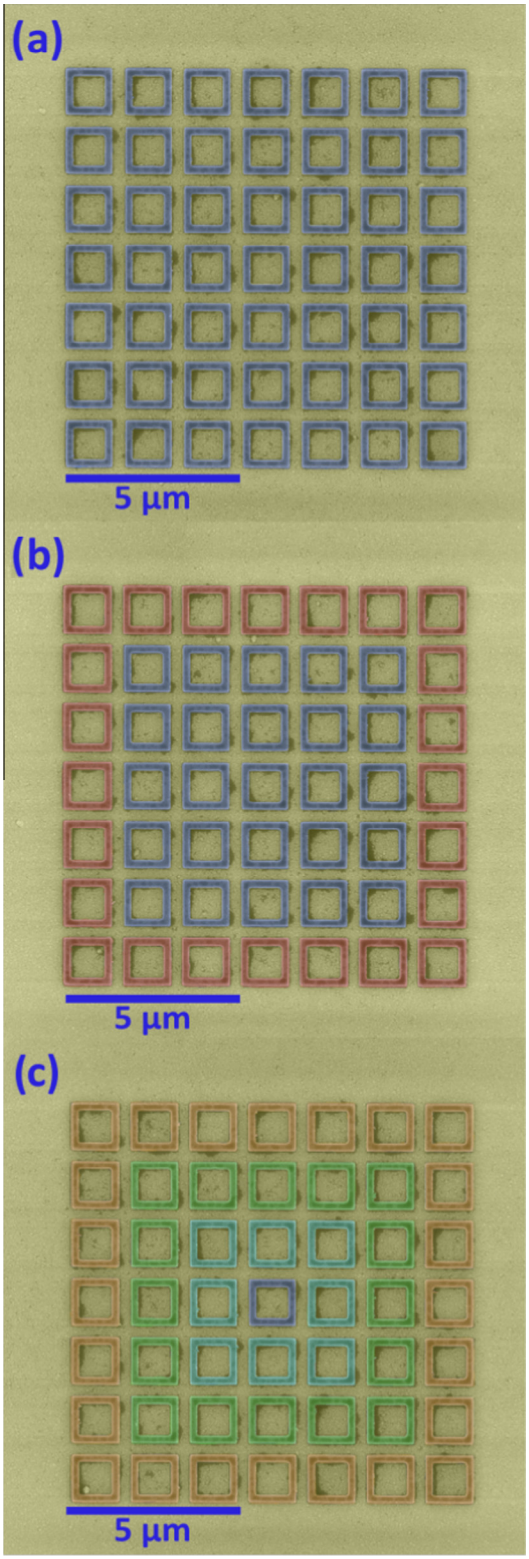

Fig. 1. False-color SEM micrographs showing the three types of finite arrays which were fabricated: (a) an unaltered 7 × 7 array of the infinite FSS design, (b) an array where the interior elements are sized according to the infinite FSS design and the perimeter elements are 50 nm larger and (c) an array where a graded increase in loop size is applied from the center loop to the perimeter.

while the unaltered 7 × 7 arrays are resonant at 9.64 μm. This behavior of blue-shifting upon truncation is consistent with that which was observed in a previous study [12]. The 7 × 7 arrays with the larger perimeter loops are seen to be resonant at 9.97 μm, while the 7 × 7 arrays with a graded size variation are seen to be resonant at 9.93 μm. Thus, the design modifications have successfully shifted the resonant wavelength of the truncated arrays approximately to that of the quasi-infinite array. It is noted that while the reported results are measured at the 60° design angle of incidence, it can be expected that these findings are applicable to other angles as well. This has been observed in both the experiments detailed here as well as a previous study [12], when comparing measurements at 60° off-normal to FTIR scans near normal incidence.

The simulated results shown in Fig. 2 are taken from calculations of the volume loss density. The volume loss density is integrated over the volume as the power absorbed by the arrays, which can be normalized to the excitation to calculate the absorptivity. Due to the opaque ground plane, the reflectivity can be plotted as unity minus the absorptivity. As can be seen in the figure, good agreement is observed between the experimental and simulated data. In all cases, the strength of resonance is observed to be stronger in the simulations, which can be attributed to the differences between the ideal simulated geometry and that which was fabricated which inherently includes surface roughness and corner curvature in the patterned structures.

The experimental and simulated data shown in Fig. 2 suggest a significant decrease in absorptivity for the truncated structures as compared to the quasi-infinite array. While array truncation may lead to some differences in absorptivity, the bulk of the perceived reduction in absorptivity stems from the difference in fill-factor between the truncated arrays and the quasi-infinite array. The square loop unit cells of the 7 × 7 arrays occupy a square area of 12.53 μm per side, and a spacing of 6.35 μm is utilized between neighboring arrays in both directions. Due to the spacing between the 7 × 7 arrays, a significant amount of open space (without square-loops) exists in the measurement area. The simulations approximate the experimental absorptivity because the spacing around each 7 × 7 array is included in the computational domain.

The experimental DDR for the quasi-infinite and 7 × 7 arrays is shown in Fig. 3. It is noted that the scale range is an order of magnitude less than that which was shown in Fig. 2. Consistent with FSS theory, since the square-loop unit cells are sufficiently sub-wavelength, the DDR of the quasi-infinite array is approximately zero. In contrast, the three patterned areas containing

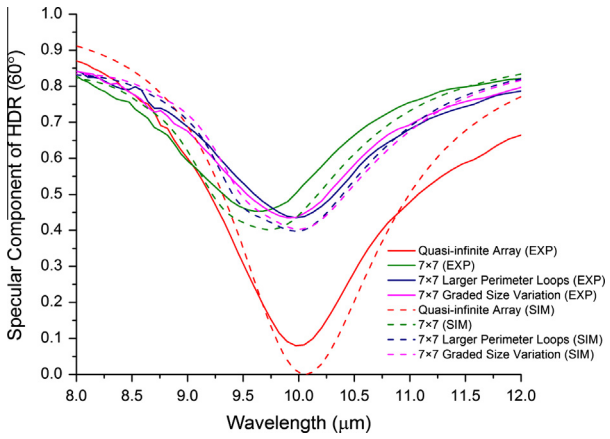

Fig. 2. Experimental and simulated SDR taken at 60° off-normal for the quasi-infinite array (red), unaltered 7 × 7 arrays (green), 7 × 7 arrays with slightly larger perimeter loops (blue), and 7 × 7 arrays with a graded size increase (magenta). Experimental resonant wavelengths are as follows: 10.02 μm for the quasi-infinite array, 9.64 μm for the unaltered 7 × 7 arrays, 9.97 μm for the 7 × 7 arrays with slightly larger perimeter loops, and 9.93 μm for the 7 × 7 arrays with a graded size increase.

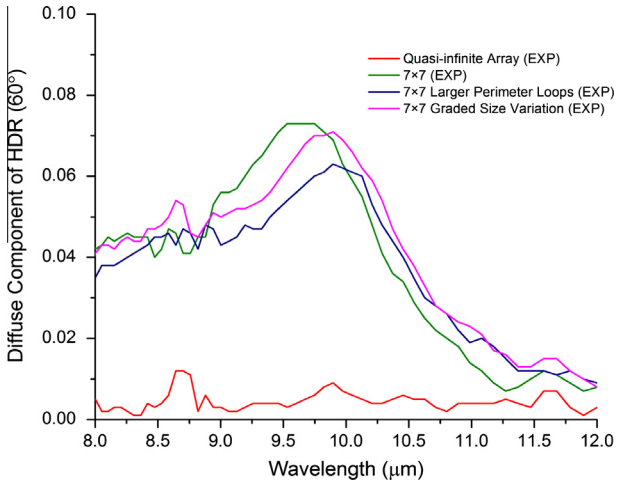

Fig. 3. Experimental DDR taken at 60° off-normal for the quasi-infinite array (red), unaltered 7 × 7 arrays (green), 7 × 7 arrays with slightly larger perimeter loops (blue), and 7 × 7 arrays with a graded size increase (magenta).

7 × 7 arrays show small but measureable DDR values near the design wavelength. Since no DDR is observed for the full array measurement, that which is observed in the measurement of the truncated arrays is attributed to diffraction effects. The diffraction occurs because the finite arrays are larger than the wavelengths of interrogation, and also because the arrays are arranged periodically on the sample to create a populated area large enough for the measurement apparatus.

5. Summary and conclusions

A square-loop infrared FSS was designed and fabricated with infinite array resonance near 10 μm at an incident angle of 60° off-normal. To demonstrate the effects of array truncation, a patterned area of finite arrays containing 7 × 7 square loops of the FSS design was fabricated. As expected from previous work, the SDR showed that the unaltered 7 × 7 arrays had a resonance which was blue-shifted from that of the infinite design. To counter the effects of truncation, two geometric modifications were made to the finite arrays. The first modification made only the perimeter loop elements slightly larger, while the second modification applied a graded loop size increase from the center of the array to the perimeter. These modified truncated arrays were measured to have resonances approximately at the resonant wavelength of the infinite FSS design.

To our knowledge, this work is the first attempt to tune the resonant wavelength of truncated arrays of FSS at infrared wavelengths. Utilizing the fact that the wavelength of resonance for a square loop is proportionally linked to its perimeter, two modified designs were shown to counteract the blue-shift in resonance brought about by array truncation. An alternative approach to the methodology shown here would be to uniformly increase the size of each square-loop in the truncated arrays. This would be equivalent to using an infinite array design which resonates at slightly longer wavelengths compared to the desired resonance of the finite arrays. In this approach, array truncation itself would blue-shift the resonance to the sought after wavelength. The advantage of the approach taken here is that the resonance of the border elements is altered, which directly affects the unit cell elements which have an electromagnetic response that is disturbed most by truncation. Tailoring the response of unit cells in truncated arrays in such a manner as presented here may benefit certain applications, such as FSS-enhanced sensors.

When tuning the response of truncated arrays by geometric modifications of the resonant unit cells, the spectral linewidth is an additional topic of interest. The current work, which altered the wavelength of peak resonance in truncated arrays by changing the size of certain square-loops, does not rigorously address the linewidth. Future work could focus on linewidth manipulation of the truncated arrays by utilizing changes in the geometry more complex than just the size of the square-loops.

Conflict of interest

The authors declare no conflict of interest.

Acknowledgments

A portion of the fabrication work was performed by D. Brown at the Georgia Tech Institute for Electronics and Nanotechnology, a member of the National Nanotechnology Infrastructure Network, which is supported by the National Science Foundation. We are thankful for the comments and suggestions of the anonymous reviewers, which have led to changes that have strengthened the clarity and quality of the manuscript.

References

[1] C.M. Rhoads, E.K. Damon, B.A. Munk, Mid-infrared filters using conducting elements, Appl. Opt. 21 (15) (1982) 2814–2816.
[2] I. Puscasu, W.L. Schaich, G.D. Boreman, Resonant enhancement of emission and absorption using frequency selective surfaces in the infrared, IR Phys. Technol. 43 (2) (2002) 101–107.
[3] J.A. Bossard, D.H. Werner, T.S. Mayer, J.A. Smith, Y.U. Tang, R.P. Drupp, L. Li, The design and fabrication of planar multiband metallodielectric frequency selective surfaces for infrared applications, IEEE Trans. Antennas Propag. 54 (4) (2006) 1265–1276.
[4] I. Puscasu, W.L. Schaich, Narrow-band, tunable infrared emission from arrays of microstrip patches, Appl. Phys. Lett. 92 (2008) 233102.
[5] J.S. Tharp, J.M. Lopez-Alonso, J.C. Ginn, C.F. Middleton, B.A. Lail, B.A. Munk, G.D. Boreman, Demonstration of a single-layer meanderline phase retarder at infrared, Opt. Lett. 31 (18) (2006) 2687–2689.
[6] J. Ginn, B. Lail, J. Alda, G. Boreman, Planar infrared binary phase reflectarray, Opt. Lett. 33 (8) (2008) 779–781.
[7] T. Maier, H. Bruckl, Wavelength-tunable microbolometers with metamaterial absorbers, Opt. Lett. 34 (19) (2009) 3012–3014.
[8] F. Alves, D. Grbovic, B. Kearney, G. Karunasiri, Microelectromechanical systems bimaterial terahertz sensor with integrated metamaterial absorber, Opt. Lett. 37 (11) (2012) 1886–1888.
[9] F. Alves, D. Grbovic, B. Kearney, N.V. Lavrik, G. Karunasiri, Bi-material terahertz sensors using metamaterial structures, Opt. Express 21 (11) (2013) 13256–13271.
[10] J.A. D' Archangel, G.D. Boreman, D.J. Shelton, M.B. Sinclair, I. Brener, Releasable infrared metamaterials, J. Vac. Sci. Technol. B 29 (5) (2011) 051806.
[11] J.A. D' Archangel, D.J. Shelton, R. Hudgins, M.K. Poutous, G.D. Boreman, Large area infrared frequency selective surface with dimensions reproducible by optical lithography, J. Vac. Sci. Technol. B 32 (5) (2014) 051807.
[12] J. D' Archangel, E. Tucker, M.B. Raschke, G. Boreman, Array truncation effects in infrared frequency selective surfaces, Opt. Express 22 (13) (2014) 16645–16659.
[13] B.A. Munk, Finite Antenna Arrays and FSS, John Wiley & Sons, 2003.